LA-UR- 04-05335

Approved for public release; distribution is unlimited.

Title: Thermodynamics of fission products in dispersion fuel designs -first-principles modeling of defect behavior in bulk and at interfaces

Author(s): X.-Y. Liu, B. P. Uberuaga, P. Nerikar, C. R. Stanek and K. E. Sickafus

Los Alamos National Laboratory, Los Alamos, NM 87545

Intended for: Journal of Nuclear Instruments and Methods in Physics Research Section B: Beam Interactions with Materials and Atoms

Los Alamos
NATIONAL LABORATORY
EST. 1943

Thermodynamics of fission products in dispersion fuel designs - first-principles modeling of defect behavior in bulk and at interfaces

X.-Y. Liu, B. P. Uberuaga, P. Nerikar, C. R. Stanek and K. E. Sickafus

Materials Science and Technology Division,

Los Alamos National Laboratory, Los Alamos, New Mexico 87545, USA

(Dated: August 11, 2009)

Abstract

Density functional theory (DFT) calculations of fission product (Xe, Sr, and Cs) incorporation and segregation in alkaline earth metal oxides, HfO_2 and UO_2 oxides, and the MgO/(U, Hf, Ce)O_2 interfaces have been carried out. In the case of UO_2, the calculations were performed using spin polarization and with a Hubbard U term characterizing the on-site Coulomb repulsion between the localized 5f electrons. The fission product solution energies in bulk $UO_{2\pm x}$ have been calculated as a function of non-stoichiometry x, and were compared to that in MgO. These calculations demonstrate that the fission product incorporation energies in MgO are higher than in HfO_2. However, this trend is reversed or reduced for alkaline earth oxides with larger cation sizes. The solution energies of fission products in MgO are substantially higher than in $UO_{2\pm x}$, except for the case of Sr in the hypostoichiometric case. Due to size effects, the thermodynamic driving force of segregation for Xe and Cs from bulk MgO to the MgO/fluorite interface is strong. However, this driving force is relatively weak for Sr.

I. INTRODUCTION

In order to close the nuclear fuel cycle, advanced concepts for separating fission products from spent nuclear fuel are necessary. One method for doing this is a dispersion fuel form, a composite in which a reprocessible inert matrix captures and immobilizes the fission products emanating from the fissile core. A critical issue of this dispersion fuel concept is the tendency of fission products to reside in one phase or another of the composite.

In this paper, we focusd on this issue in a demonstrative fuel design based on ceramic-ceramic composites. We used density functional theory (DFT) to model the defects and fission product energetics in the bulks and at interfaces. Parallel experimental efforts involving synthesis and ion irradiation studies of such composites have been recently performed as well[1]. We considered model composites in which the inert phase is MgO or another alkaline earth oxide (CaO, SrO, and BaO), all in the rock salt crystal structure. For the fissile phase, as with the experimental effort, we began with HfO_2 as a surrogate for UO_2. We also studied CeO_2 and UO_2 as the fissile phases to determine the suitability of HfO2 and CeO2 as surrogates for the true fissile UO_2. All the fissile phases considered were modelled in the fluorite crystal structure. There are numerous fission products to consider; we considered only Xe, Cs, and Sr which are rich in spent fuels. Kinetics were ignored in our calculations.

II. METHODS AND BENCHMARK

We used the efficient DFT plane-wave basis sets code VASP[2] in our calculations. The generalized gradient approximation (GGA) was used for the exchange correlation potential. Projector-augmented wave pseudopotentials were employed. For defect calculations, a 2x2x2 supercell was used with 64 atoms for alkaline earth metal oxides and 96 atoms for HfO_2 and UO_2. 2^3 k-point sampling was used in these cases. An equivalent k-point sampling was used in the interface calculations.

For systems containing UO_2, spin-polarized GGA+U method was used. In GGA+U, a Hubbard Hamiltonian that characterizes on-site Coulomb repulsion between the localized 5f electrons is used. An effective U_{eff} parameter (U-J) of 3.96 eV was used in our calculations. GGA+U predicts an insulating bandgap instead of the metallic state predicted by regular DFT for UO_2.

In Table I. the defect formation energies in MgO and UO_2 are given[3,4], in comparion with available experimental data. The computational methods correctly predict that the dominant defect in MgO is the Schottky defect, while in UO_2 it is an oxygen Frenkel pair. The formation energies are also in good agreement with experimental values, except in the case of the uranium Frenkel pair. In this case, it has been suggested that the measurement of formation energy, which was from oxygen diffusion data, is possibly underestimated[4].

III. RESULTS

A. Fission product incorporation in bulk oxides: matrix cation size effect

The incorporation energy gives the energy required to incorporate a fission product atom into a pre-existing defect site in the bulk oxide. Thus, the incorporation energy is defined as

$$E^{inc} = E_{\text{tot}} - E_{\text{trap site}} - E_{\text{fission product atom}} \tag{1}$$

where E_{tot} is the total energy of the system incorporating the fission product, $E_{\text{trap site}}$ is the energy of the defect system without the fission product, and $E_{\text{fission product atom}}$, the energy of the fission product atom at infinity, was calculated as isolated atomic contribution in a cubic supercell with 10 $\AA$ in length.

In Fig. 1, the fission products (Xe, Cs, and Sr) incorporation energies in a number of alkaline earth rocksalts (MgO, CaO, SrO and BaO) are plotted and compared with those in HfO_2. Xe and Cs are found to prefer the bound Schottky defect sites, while Sr resides on a cation vacancy. As shown in Fig. 1, it is clear that, as the cation radii of alkaline earth oxides increases, there is tendency of decreased incorporation energies for the fission product Xe and Cs. In the case of Sr, while this trend begins for MgO and CaO, when the cation size of the alkaline earth oxides increases further, the incorporation energy remains flat (in SrO) and then increases (in BaO). For Sr, the incorporation energy in the alkaline earth oxides is always higher than in HfO_2. So while the higher cation radii rocksalts might be good candidates for Xe and Cs, they may still be not good for Sr.

B. Fission product solution energies in MgO and $UO_{2\pm x}$

In calculating fission product incorporation energies, it is assumed that there are always available trap sites for the fission products. The energy costs of the formation of the trap site itself is not considered. At high burn-up, where the fission product concentratioin is high, the formation energy of the trap sites needs to be accounted for. The fission product solution energy in oxides is defined as the sum of the fission product incorporation energy plus the formation energy of the trap site. The apparent trap site formation energy was subsequently obtained through

$$E_{\text{trap site}}^{formation} = -kTln([X]) \tag{2}$$

where [X] is the defect (trap site) concentration in the system. [X] is determined from the point-defect-model (PDM) as originally introduced by Matzke[5] for non-stoichiometric $UO_{2\pm x}$.

As discussed earlier[7,8], the thermodynamic equations in PDM are,

$$[V_O][I_O] = exp(-E_{FP_O}^F/kT) \tag{3}$$

$$[V_U][I_U] = exp(-E_{FP_U}^F/kT) \tag{4}$$

$$[V_O]^2[V_U] = exp(-E_S^F/kT) \tag{5}$$

$$2[V_U] + [I_O] = 2[I_U] + 2[V_O] \pm x \tag{6}$$

where $[V_O]$, $[I_O]$, $[V_U]$ and $[I_U]$ are the concentrations of oxygen vacancies and interstitials, and uranium vacancies and interstitials respectively. $E_{FP_O}^F$,$E_{FP_U}^F$, and E_S^F are the formation energies of the oxygen and uranium Frenkel pairs and Schottky trio (Table I). Concentrations of additional trap sites in the form of divacancy Schottky and bound Schottky defects are from the relations

$$[DV] = [V_O][V_U]exp(-B_{DV}/kT) \tag{7}$$

$$[Sch] = [V_O]^2[V_U]exp(-B_{Sch}/kT) \tag{8}$$

where $[DV]$, $[Sch]$ are the concentrations of the divacancy Schottky and bound Schottky defects. B_{DV} and B_{Sch} are the binding energy of these defects (GGA+U values, 3.67 eV and 5.1 eV).

In Fig. 2, the concentrations of point defects in $UO_{2\pm x}$ at 1700 K from Eq.(4)-(7) are shown. In the hypostoichiometric (UO_{2-x}) case, the dominant point defect is the oxygen vacancy. In the hyperstoichiometric case (UO_{2+x}), the dominant point defect is the oxygen interstitial. These predictions are in excellent agreement with experimental observations.

In Fig. 3, the defect trap formation energies in the non-stoichiometric $UO_{2\pm x}$ at 1700 K are shown. The formation energy values span a wide range, from 0 - 7 eV. In the hypostoichiometric case, the oxygen vacancy has the lowest formation energy. In the hyperstoichiometric case, the divacancy Schottky defect and uranium vacancy sites have the lowest formation energies, depending on oxygen concentration. The formation energies for these lowest energy trap sites are less than 2.5 eV. In MgO, the defect trap formation energies are 3.8 eV for the bound Schottky defect and 3.15 eV for Mg vacancy. Using the incorporation energies of Xe, Cs, and Sr in UO_2[9], the solution energies in both UO_2 and MgO at 1700 K were obtained. These results are plotted in Fig. 4. Overall, the solution energies of fission products in MgO are substantially higher than those in UO_2, except for the case of Sr in hypostoichiometric UO_2, where Sr prefers the inert material over the fissile material. Since UO_2 as fuel is less likely in its hypostoichiometric state, our calculations suggest that thermodynamically, the fission products Xe, Cs, and Sr should prefer to reside in the fissile phase than in the MgO inert phase.

C. Fission product segregation at the MgO/(U, Hf, Ce)O_2 interface

In this subsection, we study the possibility of fission product segregation to the MgO/fissile phase interface. For the interface calculations, we adopted a directionally solidified eutectic interface structure for rocksalt/fluorite, as determined by high resolution TEM[10]. The original structure is of an MgO/cubic ZrO_2 interface, with the [211] direction of MgO aligned with the [100] direction of ZrO_2. The interface planes are $(1\bar{1}\bar{1})$ in MgO and (001) in ZrO_2. This same interface structure was used in our previous study of the MgO/HfO_2 interface[3].

In Fig. 5a-b, the interface structure between MgO/UO_2 is shown from two perspectives: [211] and $[01\bar{1}]$ directions in MgO. The interface structure of MgO/CeO_2 and MgO/HfO_2 are similar. The interface structure consists of eight layers of cubic UO_2 and 12 layers of MgO, with surfaces terminated with vacuum. Periodic boundary conditions were applied in

all three directions, with vacuum thickness at least 10Å. The slab model was constructed to preserve the lattice constant of MgO in the interface directions with the fluorite phase strained accordingly. To prevent cubic-tetragonal phase changes in the fluorite phase due to surface effects, the fluorite layers were kept fixed except for the two layers near the interface.

The segregation of Xe, Cs, and Sr to the rocksalt/fluorite interface was studied by calculating the segregation enthalpy of each species in its most preferred incorporation site in MgO. The segregation enthalpy is the difference in total energy between when the fission product atom is placed in the bulk-like region in MgO in the interface model, and when it is placed at the interface. At the interface region, in the case of a fission product in the bound Schottky site, there are three possible locations for the oxygen vacancy site (see Fig. 5a, labeled as A, B, C). In this case, three sets of interface calculations were carried out and the total energy of each structure after relaxation was obtained.

The results for segregation enthalpies for Xe, Cs, and Sr are summarized in Table II. For Xe substitution at a bound Schottky site, the segregation enthalpy to the interface ranges from -1.1 – -3.0 eV. For Cs, substitution at the bound Schottky site has an interfacial segregation enthalpy of -2.4 – -3.3 eV. Finally, for Sr, simple substitution for a Mg cation has an interfacial segregation enthalpy of -1.0 eV at MgO/HfO_2, and -0.3 – -0.4 eV at MgO/UO_2 and MgO/CeO_2. These results suggest that Xe and Cs will likely to segregate from bulk MgO to the MgO/fluorite interface. This is presumbly due to the large atomic sizes of Xe and Cs. However, the segregation driving force is relatively weak for Sr, which has relatively smaller atomic size.

IV. SUMMARY

DFT calculations of Xe, Sr, and Cs incorporation and segregation in alkaline earth metal oxides, HfO_2 and UO_2 oxides, and the MgO/(U, Hf, Ce)O_2 interfaces have been carried out. DFT modeling demonstrates that the fission product incorporation energies in MgO are higher than in HfO_2. However, this trend is reversed or reduced for alkaline earth oxides with larger cation sizes. The solution energies of fission products in MgO are substantially higher than in $UO_{2\pm x}$, except for the case of Sr in the hypostoichiometric case. Due to size effects, the thermodynamic driving force of segregation for Xe and Cs from bulk MgO to the MgO/fluorite interface is strong. However, such driving force is relatively weak for Sr.

The DFT results suggest that fission products considered tend to prefer the fissile phase over the inert rocksalt phase in most cases. However, there is also segregation effect for fission products from the inert MgO phase to the MgO/fluorite interface. The segregation tendency for fission products from the fissile phase to the MgO/fluorite interface is unknown. However, from another DFT study of Xe segregation from UO_2 bulk to grain-boundaries[11], it is also possible that such segregation tendency may exist.

Acknowledgments

This work was supported by the Los Alamos National Laboratory Directed Research and Development Program. LANL is operated by Los Alamos National Security, LLC, for the National Nuclear Security Administration of the U.S. Department of Energy under Contract No. DE-AC52-06NA25396.

---

[1] I.O. Usov et al., *Nucl. Instr. and Meth. B* **218** (2004), p. 451.

[2] G. Kresse and J. Hafner, *Phys. Rev. B* **47** (1993) 558; G. Kresse and J. Furthmüller, *J Comput. Mater. Sci.* **6** (1996) 15.

[3] X.-Y. Liu, B. P Uberuaga and K. E. Sickafus. *J. Phys.: Condens. Matter* **21** (2009) 045403.

[4] P. Nerikar, T. Watanabe, J. Tulenko, S. Phillpot, and S. Sinnott. *J. Nucl. Mater.* **384** (2009) 61.

[5] H. Matzke. *J. Chem. Soc., Faraday Trans.* **283** (1987) 1121.

[6] W. C. Mackrodt, in *Computer Simulation of Solids*, eds. C. R. A. Catlow and W. C. Mackrodt (Springer-Verlag, Berlin 1982), p. 175.

[7] J-P Crocombette. *J. Nucl. Mater.* **305** (2002) 29.

[8] G. Brillant and A. Pasturel, *Phys. Rev. B* **77** (2008) 184110.

[9] P. Nerikar, X.-Y. Liu, B. P Uberuaga, C. R. Stanek, S. Phillpot, and S. Sinnott, submitted.

[10] J. Echigoya, *J. Eur. Ceram. Soc.***25** (2005) 1381.

[11] P. Nerikar et al., unpublished.

TABLE I: Defect formation energies in MgO and UO_2, compared with available experimental data. MgO: magnesium and oxygen Frenkel pairs (Mg-FP and O-FP), isolated Schottky pair (Schottky), and Schottky pair in bound divacancy configuration (b-Schottky). UO_2: oxygen and uranium Frenkel pairs (O-FP and U-FP), and Schottky trio defect.

MgO defect	Mg-FP	O-FP	Schottky	b-Schottky
DFT (eV)	9.8	13.2	6.3	3.8
Expt. (eV)[6]			4 - 7	
UO_2 defect	O-FP	U-FP	Schottky trio	
DFT+U (eV)[4]	3.95	15.08	7.6	
Expt. (eV)[5]	3.0 - 4.6	8.5 - 9.6	6.0 - 7.0	

TABLE II: DFT segregation enthalpies for Xe, Cs, and Sr at MgO/(U, Hf, Ce)O_2 interface. Fission product defects are in Kröger-Vink notation. Units are in eV.

	V_O site	MgO/HfO_2	MgO/CeO_2	MgO/UO_2
$(Xe''_{Mg}{:}V_O^{\cdot\cdot})^x$	A	-3.0	-1.7	-1.3
	B	-1.9	-1.3	-1.1
	C	-1.8	-1.7	-1.3
$(Cs'_{Mg}{:}V_O^{\cdot\cdot})^{\cdot}$	A	-3.3	-3.3	
	B	-3.0	-3.3	-2.4
	C	-2.4	-3.2	
Sr^x_{Mg}	-	-1.0	-0.4	-0.3

FIG. 1: Xe, Cs, and Sr incorporation energies in alkaline earth oxides, in comparsion with in HfO_2.

FIG. 2: Point defect concentrations in $UO_{2\pm x}$: predictions from PDM model and GGA+U calculations.

FIG. 3: Defect trap formation energies at 1700 K in $UO_{2\pm x}$.

FIG. 4: Solution energies of Xe, Cs, and Sr in $UO_{2\pm x}$ in comparison with those values in MgO.

FIG. 5: (color online) MgO/UO_2 interface model. (a)-(b) final relaxed interface structure, viewed from (a) the [211] direction, (b) the $[01\bar{1}]$ direction in MgO.

Fig. 1

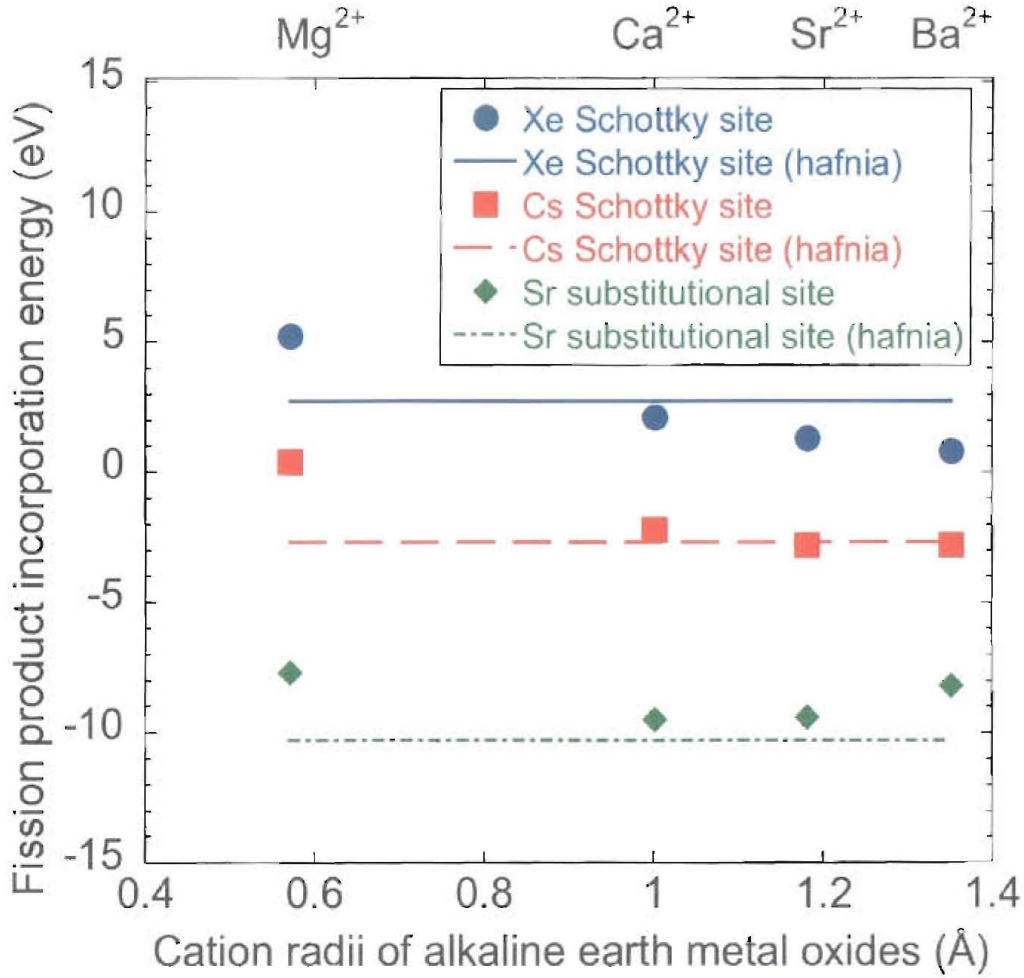
Mg2+
Ca2+
Sr2+
Ba2+
Xe Schottky site
Xe Schottky site (hafnia)
Cs Schottky site
Cs Schottky site (hafnia)
Sr substitutional site
Sr substitutional site (hafnia)
Fission product incorporation energy (eV)
15
10
5
0
-5
-10
-15
0.4
0.6
0.8
1
1.2
1.4
Cation radii of alkaline earth metal oxides (Å)

Fig. 2

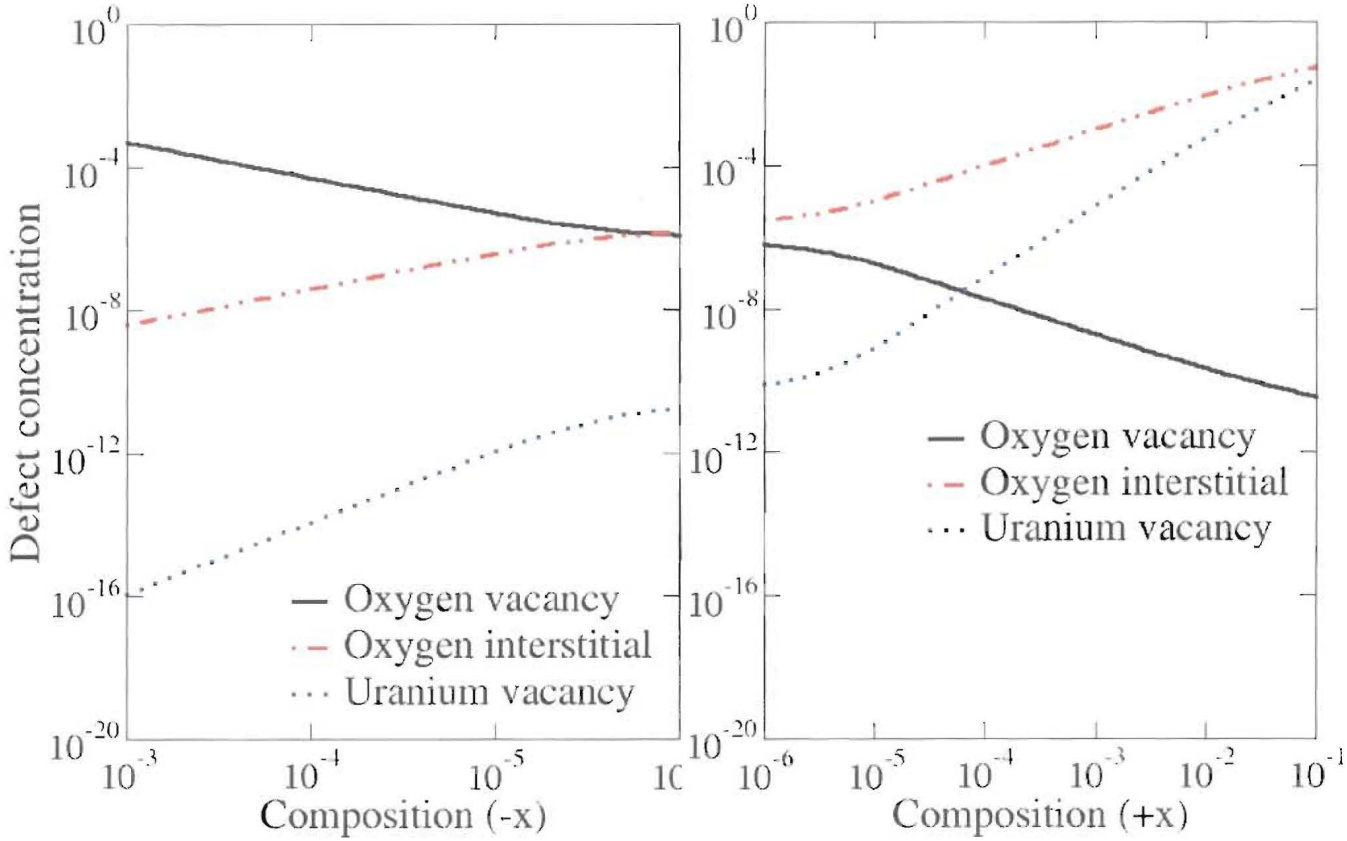
Defect concentration
Composition (-x)
Composition (+x)
Oxygen vacancy
Oxygen interstitial
Uranium vacancy

Fig. 3

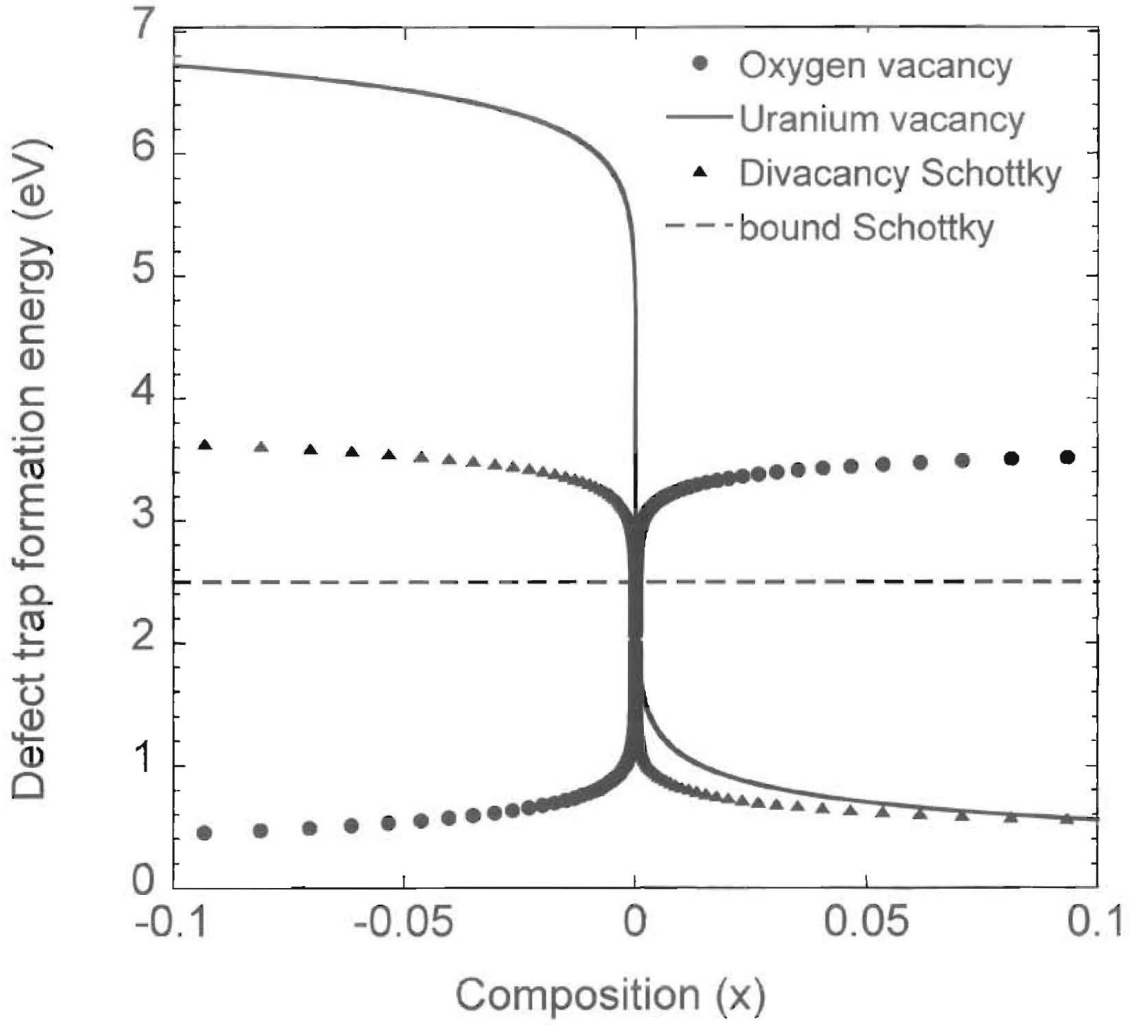
Oxygen vacancy
Uranium vacancy
Divacancy Schottky
bound Schottky
Defect trap formation energy (eV)
Composition (x)
0
1
2
3
4
5
6
7
-0.1
-0.05
0
0.05
0.1

Fig. 4

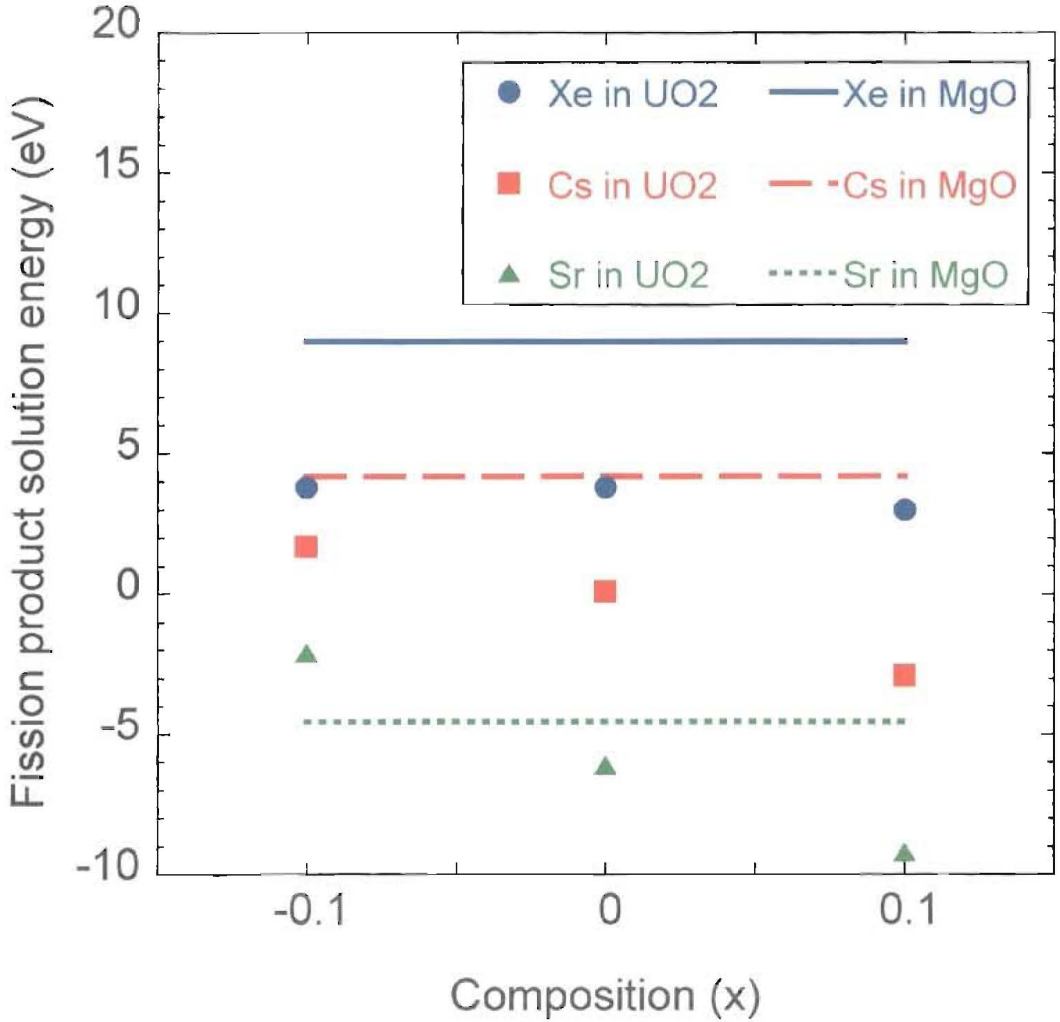
Xe in UO2
Xe in MgO
Cs in UO2
Cs in MgO
Sr in UO2
Sr in MgO
Fission product solution energy (eV)
20
15
10
5
0
-5
-10
-0.1
0
0.1
Composition (x)

Fig. 5